Atomic Structures of the Ge/Si(113)-(2×2) Surface

Zhaohui Zhang,* Koji Sumitomo,† Hiroo Omi, and Toshio Ogino
NTT Basic Research Laboratories, NTT Corporation, Atsugi, Kanagawa 243-0198, Japan

Jun Nakamura and Akiko Natori
Department of Electronic-engineering, The University of Electro-Communications, Chofu, Tokyo 182-8585, Japan
(Received 21 December 2001; published 5 June 2002)

Based on scanning tunneling microscopy observations of the epitaxial growth of Ge on Si(113) and first-principles total energy and band calculations, we demonstrate that the Ge/Si(113)-(2 × 2) surface is made up of alternating [$\bar{1}$10]-oriented rows of rebonded atoms and tilted pentamers of five atoms, where each pentamer is stabilized by an interstitial atom at the subsurface. From the existence of stacking defects in rows of tilted pentamers observed at room temperature, we have deduced that at epitaxial temperatures the pentamers frequently change their tilting orientations between two minimum energy states.

DOI: 10.1103/PhysRevLett.88.256101 PACS numbers: 68.65.La, 68.37.Ef, 68.55.Jk, 81.15.Hi

The integration of nanostructures on Si substrates has been of great interest in microelectronics for future devices for the last decade. It has been demonstrated that Ge quantum dots can be delicately assembled on Si(100) through self-organized growth [1–3], while quantum wires seem to preferably grow on Si high-index surfaces. One excellent example of the latter is elongated growth of Ge islands on Si(113) forming so-called "nanowires" [4]. For a long time studies of heteroepitaxial growth on Si have concentrated on low-index surfaces, and the growth kinetics and energies in island formation have been explained mostly in terms of the multiaxial isotropy associated with the substrates [5,6]. Recently much attention has been paid to the roles of substrate anisotropy in nanostructure self-assembly on high-index surfaces. The formation of Ge nanowires on Si(113) has challenged some theories that ignore influences of substrate anisotropy on island growth kinetics [7]. For a flat Ge film strained on Si(113), elongated growth of Ge islands on Si(113) has been attributed to effects of the anisotropic surface's stiffness on growth kinetics [8]. On the other hand, however, surface reconstruction should also play an important role in the growth process [7,9]. Si(113) with C_{1v} symmetry is well known as a stable high-index surface [10], and a 3 × 2 surface reconstruction for a clean surface has been reported by several groups [11–15]. Probably because of the epitaxial stress, the wetting layer surface changes from 3 × 2 to 2 × 2 within an initial Ge deposition of 2 ML, where 1 ML is defined as 8.2×10^{14} atoms/cm^2, and the 2 × 2 remains on the surface during the successive growth, though trenchlike defects occur when the Ge deposited is over 3 ML and Ge islanding begins when the deposition exceeds 5 ML. So far only one model for the 2 × 2 has been proposed [9], but unfortunately it is incorrect. This Letter presents our recent scanning tunneling microscopy (STM) observations to demonstrate that the 2 × 2 is actually made up of alternating [$\bar{1}$10]-oriented rows of rebonded atoms and tilted pentamers of five atoms, and each pentamer is stabilized by an interstitial atom at the subsurface. Tilting of the pentamers probably helps the Ge film to relax in the favored [$\bar{1}$10] direction and should influence further epitaxial growth.

Si(113) substrates were cut from a Si(113) wafer (phosphorus doped, 1–10 Ω cm) with a misorientation less than 0.2° away from the [113] direction. The molecular beam epitaxial growth of Ge on the Si(113) substrates was carried out with a Knudsen cell and proceeded at a rate of 1.4 ML/min. The substrate temperature was set at 430 °C during the growth, and the substrates were quenched immediately after stopping Ge deposition. The base pressure of the system was lower than 10^{-10} Torr. During Ge deposition, the pressure typically remained lower than 5×10^{-10} Torr.

A typical STM image of the surface covered with Ge of 2–3 ML is shown in Fig. 1. Two types of features line up along the [$\bar{1}$10] direction, as indicated by the arrows, forming rows, which we refer to here as *A* and *B* type for convenience. Features in an *A*-type row look lower than those in a *B*-type one, and there are depression defects in the former and protrusion defects in the latter, examples of which are enclosed by white lines. Apart from the

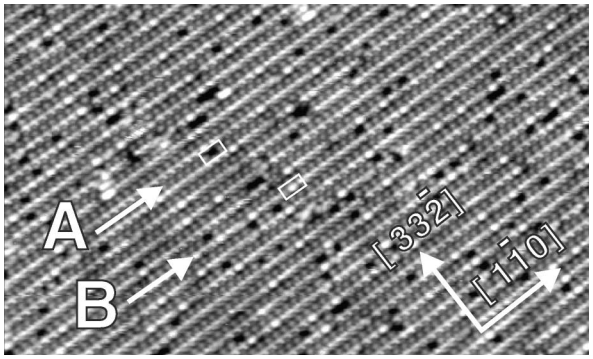

FIG. 1. An STM image of the Ge/Si(113)-(2 × 2) surface with 2-ML Ge coverage grown at 430 °C, acquired in an area of 50 × 25 nm^2 using sample voltage of −1.7 V and tunneling current of 1.5 nA.

defects, the features of *A*- and *B*-type rows arrange into a 2×2 periodicity. The atomic structure of the surface manifests itself in different configurations of the surface features, which we discuss below.

Two small-area images with an *A*- and a *B*-type row, which were cut from a pair of large STM images acquired at a same surface area, are shown in Fig. 2 to display details of the surface in filled and empty states with the sample voltages of -1.6 and $+1.6$ V, respectively. Images obtained by theoretical simulations are included and will be discussed later. The features of an *A*-type row in the filled-state image in Fig. 2(a) are marked with a circled "$-$," and between two such features a dark site is marked with a circled "$+$." In the corresponding empty-state image in Fig. 2(b), the same *A*-type row is marked with circled $-$ and $+$ at the same sites. Clearly, bright features emerge in the empty-state image at the $+$ marked sites. We measured the distance from a $-$ marked site to its neighboring $+$ marked one, and found it is just a unit length (3.84 Å) of the 1×1 surface along the $[\bar{1}10]$ direction. Nevertheless, a *B*-type row consists of a complex of bright features in both images. From the fitting of these features to pentamer blocks as the numbered circles in Fig. 2, it can be seen that sites numbered from 1 to 4 match the bright features in both images quite well. What the site numbered 5, on the other hand, indicates needs to be further discussed. In the empty-state image, it can be recognized that site 5 actually indicates a bright feature, though the contrast is weak. However, in the filled-state image, there are no features at site 5 and the next site, site 2, is much brighter than the others.

We assume that each bright feature in an empty-state image represents a surface atom. So, an *A*-type row may be made up of atoms at sites marked by the circled $-$ and $+$, and a *B*-type row may consist of atoms in pentamer blocks at sites 1 to 5. As for the difference of contrast between a $+$ marked site and a $-$ marked one, we believe that the atoms at $+$ marked sites completely lose the electron charge at their dangling bonds, resulting in no electron tunneling out at a negative sample voltage. A similar charge transfer is suggested for a pentamer block, which is tilted in a way that one side of it sinks down and the opposite side is pushed up. Since a pentamer on Si and Ge(113) is stabilized by an interstitial atom at the subsurface [11,12], it is likely that the pentamers found on Ge/Si(113) also contain such interstitials. Based on all these considerations, we propose the atomic structure for the 2×2 shown in Fig. 3. Here the features of an *A*-type row are attributed to rebonded atoms (*R* atoms) and those of a *B*-type row to tilted (*T*) pentamers of five atoms (*P* atoms) surrounding an interstitial atom (*I* atom) at the subsurface. So, we call our model TPI&R for short.

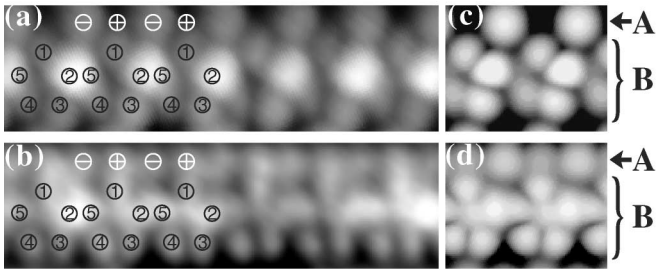

FIG. 2. Features of *A*- and *B*-type rows displayed in filled- and empty-state STM images without any defects. (a) Filled-state image at a sample voltage of -1.6 V; (b) empty-state image at 1.6 V. The tunneling current was 0.1 nA for both images. (c) and (d) Theoretically simulated images.

In order to confirm the validity of the TPI&R model, we performed first-principles total energy and band calculations [16] using a density functional method with the norm conserving pseudopotential suggested by Troullier and Martins [17]. Exchange and correlation were treated with a generalized gradient approximation (GGA) [18]. The wave function was expanded in a plane-wave basis set with a kinetic-energy cutoff of 16 (up to 20) Ry. Brillouin zone integration was done at 16 *k* points in the two-dimensional zone, and structures were optimized by a conjugate gradient method. The slab model used was 2 ML of Ge on 3 ML of Si and the backside of the slab was terminated with H atoms [19]. It was assumed that no intermixing occurs at the interface between Ge and Si [20]. From the calculations, we found that our TPI&R model has a surface energy of -2.0 eV per 2×2 unit cell relative to the bulk-truncated surface, which is lower by 1.2 eV relative to the model proposed by Knall *et al.* [9]. It was also determined that the existence of *I* atoms in the TPI&R structure lowers the surface energy by 0.4 eV, compared with the same pentamer structure but without any interstitials. Besides, the surface is semiconducting and the energy gap is 0.4 eV.

The optimized TPI&R configuration of the 2×2 was also determined. The z coordinates of the *R* atoms, $Z_{(R+)}$

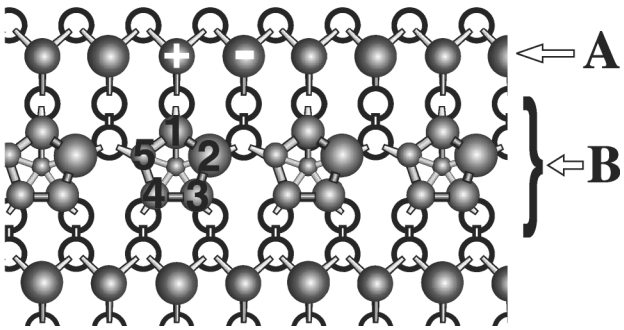

FIG. 3. The TPI&R model consisting of tilted (*T*) pentamers (*P*) stabilized by interstitial atoms (*I*) and rebonded atoms (*R*). The *R* atoms, arrow *A*, are presented in two different sizes to indicate their two different states. The *P* atoms, arrow *B*, are presented in different sizes to display the tilted configuration of the pentamers in that larger atoms are higher than smaller ones. The *I* atoms are located at the subsurface underneath the pentamers. The open circles represent sites of bulk-truncated atoms.

TABLE I. Z coordinates of the surface atoms (Å).

$Z_{(R+)}$	$Z_{(R-)}$	$Z_{(P1)}$	$Z_{(P2)}$	$Z_{(P3)}$	$Z_{(P4)}$	$Z_{(P5)}$
−1.66	−0.63	−0.27	0	−0.24	−0.52	−0.76

and $Z_{(R-)}$, and the P atoms, $Z_{(Pi)}$ ($i = 1, 2, 3, 4, 5$; see numbers in Fig. 3), are listed in Table I. Clearly, the + marked R atoms are about 1 Å lower than those marked with a −, and the different heights of the P atoms indicate that the pentamers are really tilted. Careful examination showed that the five atoms of a pentamer are not in a plane. So, the pentamers are tilted and puckered. The angle between the surface and the tilt direction from the highest atom to the lowest one is about 10°, which may be considered as a characteristic amount for a tilted pentamer. Not all the bond lengths between two neighboring atoms in a pentamer are equal, as listed under $L_{(Pi-Pj)}$ in Table II, but the I atom is bonded with each P atom at the same length denoted by $L_{(I-Px)}$, that is, 2.60 Å.

The aforementioned STM images Figs. 2(c) and 2(d) were simulated based on an optimized TPI&R structure from first-principles calculations using the Tersoff-Hamann formalism [21]. They qualitatively agree with the experiments, and show clearly why the STM images in filled and empty states appear so different. The reason is simply charge transfer of electrons from the lower atoms to the higher ones during the TPI&R structure formation, which results from the stronger electronegativity of the higher atoms [22–24]. The resulting redistribution of electron charge on the surface tends to make dangling bonds of the lower atoms empty and those of the upper atoms completely filled. Consequently, there are almost no unsaturated dangling bonds at the surface. So, corrugation of the atomic structure is enhanced in a filled-state STM image but weakened in an empty one. Moreover, the change in the dangling orbital forces its states to shift into the conduction or valence band, so that there are no dangling bond states in the energy band gap. The stability of our TPI&R model is therefore directly attributed to the semiconducting nature of the surface, which is originated from a kind of Jahn-Teller effect [25].

From lowering surface energy, our calculations indicate the existence of I atoms. Experimental evidence of I atoms, on the other hand, is found in the I-atom-missing defects observed in B-type rows. As can be seen in Fig. 4, new blocks of features emerge in B-type rows (arrows). Four bright spots in the empty-state image are marked with four closed circles. In the filled-state image, however, two of them seem to sink down (stars). Especially, unlike a pentamer, there is no bright feature at the site marked by an open circle. Such configurations suggest that this is just a puckered tetramer as has been proposed for the Si(113)-3 × 2 reconstruction [13], in which one of two dimerized atoms is buckled downward and the other upward, causing their adjacent two (111)-like atoms to buckle in opposite directions, respectively. The number ratio of tetramer to pentamer was measured to be less than 7% when the Ge coverage is not thinner than 2 ML. So, a tetramer occurs on the 2 × 2 surface as a defect where an I atom is missing, which makes the existence of the pentamer structure unambiguous.

TABLE II. Bond lengths between two neighboring atoms in a pentamer with an interstitial atom at the subsurface (Å).

$L_{(P1-P2)}$	$L_{(P2-P3)}$	$L_{(P3-P4)}$	$L_{(P4-P5)}$	$L_{(P5-P1)}$	$L_{(I-Px)}$
2.60	2.60	2.48	2.40	2.48	2.60

Now that the 2 × 2 surface reconstructs into the TPI&R structure, the depression and protrusion defects pointed out in Fig. 1 become understandable. In Fig. 4, we pointed out that depression defects of A-type rows result from missing R atoms. We show highly magnified protrusion defect of a B-type row in Fig. 5 (encircled). According to the determination of the TPI&R structure, it is found that the pentamers are tilted in opposite directions on both sides of a protrusion defect, as marked by closed and open circles in Fig. 5. So, such a protrusion defect actually results from the meeting of the upper sides of two oppositely tilted pentamers. We also observed that, as the tip was scanned, pentamers near defects of B-type rows alternate between two tilted configurations or between a flat and a tilted configuration. The distribution of the pentamers tilted in phase locally may indicate locally collective orientation of the pentamers when the Ge deposition was interrupted and the sample quenched, which would leave the pentamers at the boundaries unstable. Nevertheless, at the epitaxial temperature all pentamers may have changed their orientation frequently between two minimum energy states of two oppositely tilting orientations. Interestingly, an interstitial atom was found to stay at the subsurface and bring five surface atoms together in a tilted pentamer block.

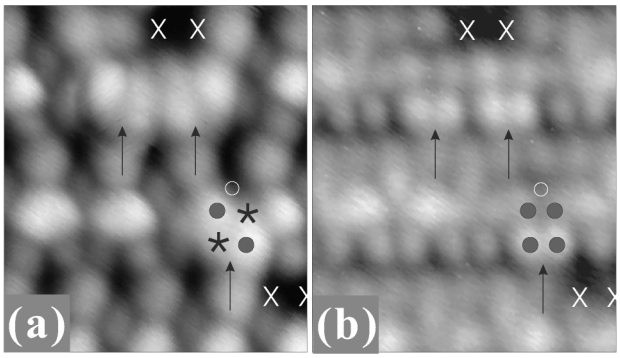

FIG. 4. Features of tetramers without subsurface I atoms: Three tetramer blocks are indicated with arrows and the features of one block marked with closed circles and stars. The open circles mark a surface vacancy, indicating a missing interstitial atom. The X's mark vacancies of R atoms, namely, depression defects of A-type rows. (a) Filled STM image at sample voltage of −1.9 V; (b) empty STM image at sample voltage of 1.9 V. The tunneling current for both images was 0.1 nA.

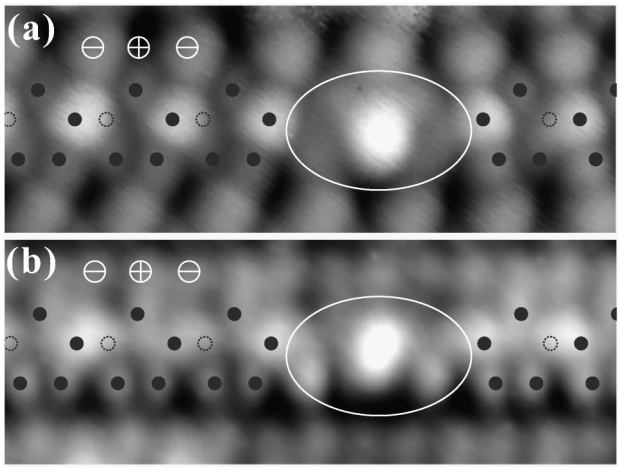

FIG. 5. Protrusion defect of *B*-type rows in filled- and empty-state images. (a) Filled STM image at sample voltage of −1.9 V; (b) empty STM image at sample voltage of 1.9 V. The tunneling current for both images was 0.1 nA.

In summary, the Ge/Si(113)-(2 × 2) surface is made up of alternating $[\bar{1}10]$-oriented rows of rebonded atoms and tilted pentamers of five atoms, and each one of the pentamers is stabilized by an interstitial atom at the subsurface. We also find that, in order to lower the surface stress, caused by the 4% lattice mismatch between Ge and Si, the most energetically favorable configuration is achieved by the lining up of the *R* atoms and a tilt of the pentamers along the $[\bar{1}10]$ direction. These surface relaxation effects should influence further growth, leading to the formation of trenchlike defects and nanowires across the $[\bar{1}10]$, although the quantitative analysis is not easy and complete understanding is yet to be made. We believe that such unique surface reconstruction resulting in anisotropic surface strain can play a crucial role in deciding the nature of growth on these high-index surfaces.

*Present address: Mesoscopic Physics National Laboratory and Department of Physics, Peking University, Beijing 100871, China.
†Corresponding author.
Email address: sumitomo@will.brl.ntt.co.jp

[1] Y.-W. Mo *et al.,* Phys. Rev. Lett. **65**, 1020 (1990).
[2] G. Medeiros-Ribeiro *et al.,* Science **279**, 353 (1998).
[3] F. M. Ross, R. M. Tromp, and M. C. Reuter, Science **286**, 1931 (1999).
[4] H. Omi and T. Ogino, Appl. Phys. Lett. **71**, 2163 (1997); Phys. Rev. B **59**, 7521 (1999).
[5] J. Tersoff and R. M. Tromp, Phys. Rev. Lett. **70**, 2782 (1993).
[6] A. Li, F. Liu, and M. G. Lagally, Phys. Rev. Lett. **85**, 1922 (2000).
[7] D. J. Bottomley, H. Omi, and T. Ogino, J. Cryst. Growth **225**, 16 (2001).
[8] Z. Zhang *et al.,* Surf. Sci. **497**, 93 (2002).
[9] J. Knall and J. B. Pethica, Surf. Sci. **265**, 156 (1992).
[10] D. J. Eaglesham *et al.,* Phys. Rev. Lett. **70**, 1643 (1993).
[11] J. Dąbrowski, H.-J. Müssig, and G. Wolff, Phys. Rev. Lett. **73**, 1660 (1994); J. Vac. Sci. Technol. B **13**, 1597 (1997).
[12] A. Laracuente, S. C. Erwin, and L. J. Whitman, Phys. Rev. Lett. **81**, 5177 (1998).
[13] J. Wang *et al.,* Phys. Rev. B **54**, 13 744 (1996).
[14] C. Y. Chang *et al.,* Phys. Rev. Lett. **83**, 2580 (1999).
[15] C. Y. Chang, Y. C. Chou, and C. M. Wei, Phys. Rev. B **59**, R10 453 (1999).
[16] M. Tsukada *et al.,* computer program package TAPP, University of Tokyo, Tokyo, Japan, 1983–2001.
[17] N. Troullier and J. L. Martins, Phys. Rev. B **43**, 1993 (1991).
[18] J. P. Perdew, K. Burke, and Y. Wang, Phys. Rev. B **54**, 16 533 (1996).
[19] In order to check the validity of the thickness in the repeated slab model, we employed a supercell containing 4 and 2 ML of Si and Ge, respectively. It was found that a supercell containing 3 ML of Si is sufficient to achieve the convergence of energy differences within ~0.02 eV per 2 × 2 unit cell.
[20] We observed the same 2 × 2 structure not only on the wetting layer surface but also on top of epitaxial islands, and also found that intermixing of Ge and Si at a low temperature of 400 °C was not severe. Using a medium-energy ion scattering technique, we confirmed that there were no Si atoms in the topmost layer of 2 × 2 surface with 4-ML-thick Ge. Therefore, we can conclude that Si atoms diffusing into the Ge film is not the reason for the reconstruction observed.
[21] J. Tersoff and D. R. Hamann, Phys. Rev. B **31**, 805 (1985).
[22] A. Ohtake *et al.,* Phys. Rev. B **64**, 045318 (2001).
[23] J. Nakamura *et al.,* J. Phys. Soc. Jpn. **66**, 1656 (1997).
[24] J. Nakamura, H. Nakajima, and T. Osaka, Appl. Surf. Sci. **121/122**, 249 (1997).
[25] T. Hitosugi *et al.,* Phys. Rev. Lett. **82**, 4034 (1999).